

Towards Gold-Standard Depth Estimation for Tree Branches in UAV Forestry: Benchmarking Deep Stereo Matching Methods

Yida Lin, Bing Xue, Mengjie Zhang

Centre for Data Science and Artificial Intelligence

Victoria University of Wellington, Wellington, New Zealand

linyida@myvuw.ac.nz, bing.xue@vuw.ac.nz, mengjie.zhang@vuw.ac.nz

Sam Schofield, Richard Green

Department of Computer Science and Software Engineering

University of Canterbury, Canterbury, New Zealand

sam.schofield@canterbury.ac.nz, richard.green@canterbury.ac.nz

Abstract—Autonomous UAV forestry operations require robust depth estimation with strong cross-domain generalization, yet existing evaluations focus on urban and indoor scenarios, leaving a critical gap for vegetation-dense environments. We present the first systematic zero-shot evaluation of eight stereo methods spanning iterative refinement, foundation model, diffusion-based, and 3D CNN paradigms. All methods use officially released pretrained weights (trained on Scene Flow) and are evaluated on four standard benchmarks (ETH3D, KITTI 2012/2015, Middlebury) plus a novel 5,313-pair Canterbury Tree Branches dataset (1920×1080). Results reveal scene-dependent patterns: foundation models excel on structured scenes (BridgeDepth: 0.23 px on ETH3D; DEFOM: 4.65 px on Middlebury), while iterative methods show variable cross-benchmark performance (IGEV++: 0.36 px on ETH3D but 6.77 px on Middlebury; IGEV: 0.33 px on ETH3D but 4.99 px on Middlebury). Qualitative evaluation on the Tree Branches dataset establishes DEFOM as the gold-standard baseline for vegetation depth estimation, with superior cross-domain consistency (consistently ranking 1st–2nd across benchmarks, average rank 1.75). DEFOM predictions will serve as pseudo-ground-truth for future benchmarking.

Index Terms—Stereo matching, depth estimation, cross-domain generalization, UAV applications, autonomous forestry

I. INTRODUCTION

Radiata pine (*Pinus radiata*) is New Zealand’s dominant plantation species, with forestry contributing NZ\$3.6 billion (1.3%) to national GDP. Regular pruning is essential for high-quality clear-wood production, yet manual operations pose significant hazards including falls and chainsaw injuries. Autonomous UAV-based pruning offers a safer alternative [12], [13], but requires centimeter-level depth accuracy for precise tool positioning at 1–2 m operating distances. Recent advances have demonstrated the potential of integrating object detection with stereo vision [14], deep learning for branch segmentation [15], and evolutionary optimization for stereo matching [16]. Unlike urban or indoor scenes, forest canopies feature thin overlapping branches, repetitive patterns, extreme depth discontinuities, and dramatic illumination variations. Stereo vision provides a passive, lightweight alternative to power-hungry active sensors, ideal for resource-constrained aerial platforms.

Deep learning has advanced stereo matching significantly through end-to-end trainable architectures. The Scene Flow dataset [1] has become the de facto standard for pretraining,

providing over 39,000 synthetic stereo pairs with dense, pixel-perfect ground-truth disparity—annotations that are impractical to obtain at scale in real-world scenes. Our goal is to identify the most robust pretrained model for generating pseudo-ground-truth on our Tree Branches dataset, which comprises 5,313 high-quality stereo pairs captured using a ZED Mini camera mounted on a UAV. Since no LiDAR annotation exists, we evaluate models through zero-shot inference on established benchmarks—KITTI [8], Middlebury [10], and ETH3D [11]—using Scene Flow pretrained weights without any fine-tuning. Based on cross-domain generalization performance, we then select the most robust method to generate gold-standard pseudo-ground-truth for our Tree Branches dataset. Inference speed is not considered, as our focus is purely on prediction quality.

Three gaps motivate this study. *First*, existing stereo benchmarks (KITTI, ETH3D, Middlebury) focus on automotive and indoor scenarios, providing limited insight for vegetation-dense environments. *Second*, most comparative studies permit domain-specific fine-tuning, obscuring the pure generalization capability essential when target-domain annotations—like LiDAR depth maps in dense canopies—are unavailable. *Third*, the relative performance of recent paradigms—iterative refinement, foundation models, and diffusion-based methods—remains unclear for cross-domain deployment in forestry applications.

To address these gaps, we evaluate eight deep stereo methods spanning four architectural paradigms: iterative refinement (RAFT-Stereo [2], IGEV [3], IGEV++ [4]), foundation models (BridgeDepth [5], DEFOM-Stereo [7], hereafter DEFOM), diffusion-based (StereoAnywhere [6]), and 3D CNN (ACVNet [24], PSMNet [22]). All methods use Scene Flow pretrained weights and are evaluated zero-shot on four standard benchmarks plus our 5,313-pair Tree Branches dataset. Our contributions are:

- **Systematic paradigm comparison:** The first zero-shot evaluation comparing iterative refinement, foundation models, diffusion-based, and 3D CNN methods under identical training conditions to isolate inherent generalization capability for forestry deployment.
- **Comprehensive cross-domain evaluation:** Consistent

assessment on four standard benchmarks spanning indoor, automotive, and high-resolution scenarios.

- **Performance analysis:** Quantitative comparison revealing scene-dependent patterns—foundation models excel on structured scenes while iterative methods show variable cross-benchmark robustness—informing method selection for vegetation-specific applications.
- **Gold-standard baseline for forestry:** DEFOM identified as optimal for the Tree Branches dataset based on superior cross-domain consistency (average rank 1.75 across benchmarks), enabling future quantitative benchmarking with pseudo-ground-truth depth maps.

II. RELATED WORK

A. Deep Stereo Matching Architectures

Deep learning has transformed stereo matching through end-to-end trainable architectures. Early 3D CNN methods established the foundation: DispNet [1] demonstrated end-to-end disparity regression, GC-Net [21] introduced 3D convolutions for cost volume regularization, and PSMNet [22] incorporated spatial pyramid pooling for multi-scale context aggregation. ACVNet [24] advanced this paradigm with attention-based cost volume construction. While effective on training domains, these methods struggle with large disparity ranges and cross-domain transfer—a critical limitation for forestry applications where Scene Flow training data differs substantially from vegetation scenes.

Iterative refinement methods, inspired by optical flow estimation, address these limitations through progressive disparity updates. RAFT-Stereo [2] adapts recurrent all-pairs field transforms with multi-scale correlation volumes. IGEV [3] combines iterative updates with geometry encoding volumes to handle occlusions and textureless regions. IGEV++ [4] extends this with multi-range geometry encoding for large disparities while preserving fine-grained details—potentially beneficial for capturing thin branch structures in forestry scenes.

B. Foundation Models and Diffusion-Based Methods

Recent foundation model approaches exploit large-scale pre-training and monocular depth priors to enhance cross-domain generalization. BridgeDepth [5] bridges monocular contextual reasoning and stereo geometric matching through iterative bidirectional alignment in latent space. DEFOM-Stereo [7] incorporates Depth Anything V2 into recurrent stereo matching with scale update modules, leveraging monocular depth priors trained on diverse real-world scenes. These methods are particularly promising for forestry applications where monocular cues can resolve ambiguities in textureless foliage regions.

Diffusion-based paradigms offer an alternative approach to cross-domain transfer. StereoAnywhere [6] formulates stereo matching as conditional image generation, enabling zero-shot transfer through learned image priors. However, systematic comparison of these paradigms—iterative refinement, foundation models, and diffusion-based methods—under identical zero-shot conditions remains limited, particularly for vegetation-dense environments.

C. Stereo Vision for UAV Forestry

UAV-based stereo vision has been explored for navigation [25], 3D reconstruction [26], and obstacle avoidance [27]. However, most systems target structured urban environments, leaving forestry applications underexplored. Forest canopies present unique challenges for stereo matching: thin overlapping branches require fine-grained depth resolution, repetitive foliage patterns create ambiguous correspondences, extreme depth discontinuities challenge cost aggregation, and variable natural illumination causes appearance changes between stereo views.

While monocular depth has been applied to forest inventory [28], stereo-based approaches offer geometric constraints essential for precise depth estimation at close range (1–2 m) required for autonomous pruning operations. Recent work on branch detection [13], [14] and segmentation [15] has demonstrated the potential of integrating deep learning with stereo vision for forestry, but relies on classical matching methods. Evaluating modern deep stereo architectures for vegetation scenes remains an open challenge.

D. Zero-Shot Cross-Domain Generalization

Domain adaptation in stereo matching typically employs supervised fine-tuning [29] or self-supervised adaptation [30], but requires target-domain data—often impractical for forestry where dense ground-truth acquisition via LiDAR is hindered by canopy occlusion. Zero-shot generalization—deploying models trained solely on synthetic data—offers a practical alternative.

The Scene Flow dataset [1] has become the de facto standard for pre-training, providing dense ground-truth unavailable at scale in real-world scenes. Existing benchmarks (KITTI [8], ETH3D [11], Middlebury [10]) enable cross-domain evaluation but focus on automotive and indoor scenarios, providing limited insight for vegetation-dense environments. Our work addresses this gap through systematic zero-shot evaluation across diverse benchmarks plus a novel forestry dataset, identifying optimal methods for generating pseudo-ground-truth where LiDAR annotation is infeasible.

III. METHODOLOGY

A. Problem Formulation

Stereo matching estimates per-pixel disparity from a rectified stereo image pair. Given left and right images $I_L, I_R \in \mathbb{R}^{H \times W \times 3}$, the goal is to compute a disparity map $D \in \mathbb{R}^{H \times W}$ where each pixel (x, y) in the left image corresponds to pixel $(x - D(x, y), y)$ in the right image. The depth Z at pixel (x, y) can be recovered through triangulation:

$$Z(x, y) = \frac{f \cdot B}{D(x, y)} \quad (1)$$

where f is the focal length and B is the stereo baseline. Deep stereo methods learn a mapping $f_\theta : \mathbb{R}^{H \times W \times 3} \times \mathbb{R}^{H \times W \times 3} \rightarrow \mathbb{R}^{H \times W}$ parameterized by weights θ , trained to minimize disparity prediction error on labeled data.

B. Datasets

We evaluate stereo matching methods across five diverse datasets to assess generalization capability:

Scene Flow [1] provides over 39,000 synthetic stereo pairs with perfect ground-truth for training.

ETH3D [11] contains high-resolution indoor/outdoor pairs with structured-light ground-truth.

KITTI 2012/2015 [8], [9] represent autonomous driving scenarios with LiDAR ground-truth.

Middlebury [10] provides high-accuracy indoor ground-truth for fine-grained disparity estimation.

Tree Branches Dataset: We introduce 5,313 stereo pairs (1920×1080) captured using a ZED Mini camera (63 mm baseline) mounted on a UAV in Canterbury, New Zealand (March–October 2024). Pairs were rigorously selected from hundreds of thousands of raw captures through multi-stage filtering assessing motion blur, exposure quality, stereo rectification accuracy, and scene diversity. The dataset targets vegetation-specific challenges: thin overlapping branches, repetitive foliage patterns, extreme depth discontinuities, and variable illumination. *No ground-truth depth maps are provided.* The dataset will be publicly released with DEFOM pseudo-ground-truth to facilitate UAV forestry research.

C. Evaluated Methods

We first survey 20 representative deep stereo methods using their officially released pretrained weights and evaluate them on KITTI 2015 and Middlebury benchmarks (Fig. 1). Based on this initial screening, we select eight methods spanning different architectural paradigms for comprehensive cross-domain generalization evaluation (Table I). Selection criteria include: (1) competitive performance on at least one benchmark, (2) coverage of diverse architectural paradigms, and (3) availability of Scene Flow pretrained weights for fair comparison.

TABLE I: Evaluated Stereo Matching Methods and Their Architectural Paradigms

| Method | Type | Key Feature |
|--------------------|------------|----------------------------|
| RAFT-Stereo [2] | Iterative | Recurrent field transforms |
| IGEV [3] | Iterative | Geometry encoding volume |
| IGEV++ [4] | Iterative | Multi-range encoding |
| BridgeDepth [5] | Foundation | Latent alignment |
| DEFOM [7] | Foundation | Depth foundation model |
| StereoAnywhere [6] | Diffusion | Zero-shot transfer |
| ACVNet [24] | 3D CNN | Attention concatenation |
| PSMNet [22] | 3D CNN | Spatial pyramid pooling |

D. Evaluation Metrics

We employ two complementary metrics that capture different aspects of stereo matching quality. **End-Point Error (EPE)** measures the average absolute disparity error:

$$EPE = \frac{1}{N} \sum_{i=1}^N |d_i - \hat{d}_i| \quad (2)$$

EPE reflects overall prediction accuracy and is sensitive to systematic bias, making it suitable for assessing methods intended as pseudo-ground-truth baselines. **D1-Error** computes the percentage of pixels with error exceeding 3 pixels:

$$D1 = \frac{1}{N} \sum_{i=1}^N \mathbb{1}(|d_i - \hat{d}_i| > 3) \quad (3)$$

D1 captures the proportion of catastrophic failures independent of error magnitude, critical for safety applications where consistent reliability matters more than mean accuracy.

For UAV forestry, EPE directly relates to depth accuracy: sub-pixel disparity errors translate to centimeter-level depth precision. D1 identifies regions of complete matching failure common in vegetation scenes. Together, these metrics distinguish methods with consistent performance from those with high failure rates.

E. Implementation Details

Pre-trained Models: All methods use officially released Scene Flow weights [1] with zero-shot inference.

Evaluation Protocol: Experiments are conducted on an NVIDIA Quadro RTX 6000 GPU (24 GB VRAM) with PyTorch 2.6.0. We use full-resolution images without cropping. Invalid pixels are excluded following standard protocols. For stochastic methods, we report means across three runs.

IV. EXPERIMENTAL RESULTS

A. Performance on Standard Benchmarks

Table II summarizes zero-shot results on four standard benchmarks.

1) *Performance Analysis by Method: Foundation Models (BridgeDepth, DEFOM):* Both methods leverage monocular depth priors from large-scale pretraining. BridgeDepth achieves best results on ETH3D (0.23 px EPE, 0.39% D1) and KITTI (0.83 px on KITTI 2012, 3.65% D1), but degrades significantly on Middlebury (20.03 px EPE, 19.54% D1). This suggests BridgeDepth’s latent alignment works well within moderate disparity ranges but struggles with Middlebury’s extreme disparities. DEFOM shows more balanced performance: competitive on ETH3D (0.35 px) and KITTI (0.84 px on KITTI 2012, 1.04 px on KITTI 2015), while achieving best EPE on Middlebury (4.65 px). DEFOM’s scale update modules enable adaptation to varying disparity ranges.

Iterative Methods (RAFT-Stereo, IGEV, IGEV++): These methods show moderate and consistent performance. RAFT-Stereo achieves 0.27 px on ETH3D and 0.90 px on KITTI 2012. IGEV performs similarly (0.33 px on ETH3D, 1.03 px on KITTI 2012) but achieves best D1 on Middlebury (6.79%). IGEV++ shows slightly higher errors (0.36 px on ETH3D, 1.20 px on KITTI 2012), indicating that additional complexity does not always improve generalization.

Diffusion-Based (StereoAnywhere): Moderate performance across benchmarks (0.43 px on ETH3D, 1.02 px on KITTI 2012, 9.51 px on Middlebury). The diffusion formulation provides reasonable zero-shot transfer but does not outperform foundation models or iterative methods.

Performance Comparison: Middlebury vs KITTI 2015

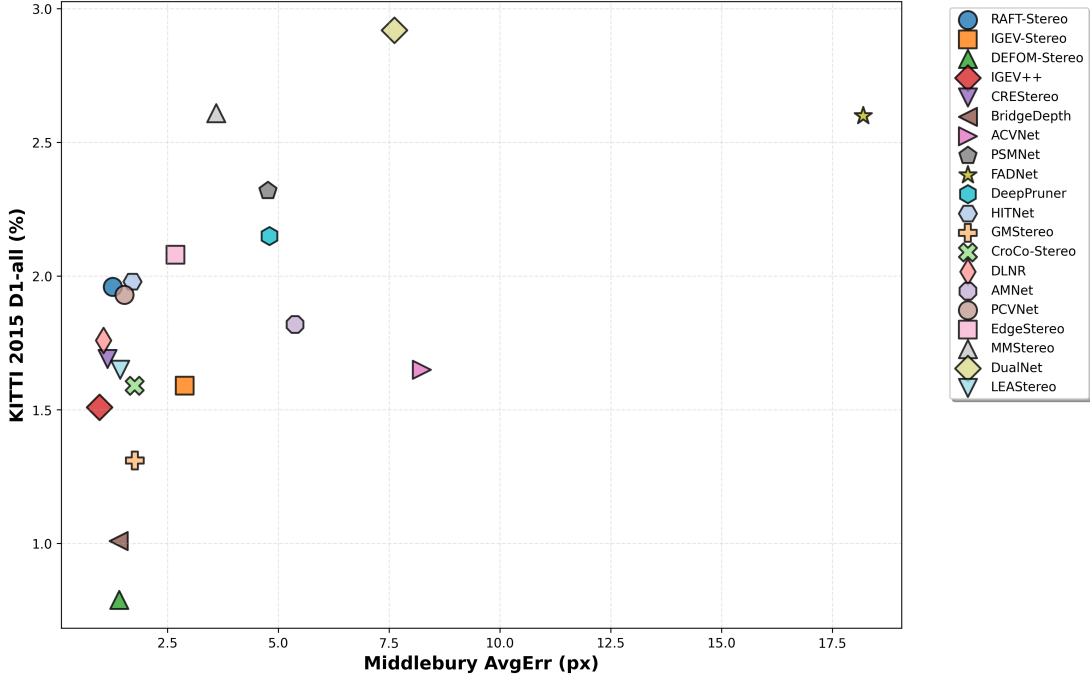


Fig. 1: Initial screening of 20 stereo matching methods using officially released pretrained weights on KITTI 2015 (D1-all %) and Middlebury (Average Absolute Error, pixels). Foundation models (DEFOM: 0.79% D1, BridgeDepth: 1.01% D1) dominate KITTI 2015, while iterative methods (IGEV++: 0.97 px AAE, DLNR: 1.06 px) excel on Middlebury. Based on this screening, eight methods (highlighted) are selected for comprehensive cross-domain generalization evaluation, balancing performance and architectural diversity. Classical 3D CNN methods (ACVNet, PSMNet) are included as baselines despite higher errors.

TABLE II: Cross-Domain Generalization Performance on Standard Benchmarks

| Method | ETH3D | | KITTI 2012 | | KITTI 2015 | | Middlebury | |
|----------------|------------------|-----------------|------------------|-----------------|------------------|-----------------|------------------|-----------------|
| | EPE \downarrow | D1 \downarrow |
| RAFT-Stereo | 0.27 | 0.88 | 0.90 | 4.41 | 1.11 | 5.12 | 5.50 | 10.80 |
| IGEV | 0.33 | 1.44 | 1.03 | 5.21 | 1.17 | 5.45 | 4.99 | 6.79 |
| IGEV++ | 0.36 | 1.70 | 1.20 | 6.37 | 1.23 | 5.83 | 6.77 | 7.82 |
| BridgeDepth | 0.23 | 0.39 | 0.83 | 3.65 | 1.07 | 4.34 | 20.03 | 19.54 |
| StereoAnywhere | 0.43 | 2.04 | 1.02 | 4.91 | 1.11 | 5.43 | 9.51 | 18.84 |
| DEFOM | 0.35 | 0.92 | 0.84 | 3.76 | 1.04 | 4.57 | 4.65 | 8.28 |
| ACVNet | 1.95 | 3.50 | 1.91 | 11.72 | 2.18 | 9.95 | 37.36 | 36.67 |
| PSMNet | 2.15 | 4.20 | 3.77 | 27.32 | 3.97 | 28.21 | 48.62 | 54.42 |

EPE: End-Point Error (pixels), D1: Percentage of pixels with error >3 px (%). All methods use Scene Flow pretrained weights without fine-tuning. Bold indicates best per benchmark.

Classical 3D CNN (ACVNet, PSMNet): Both methods fail significantly across all benchmarks. ACVNet shows 1.95 px on ETH3D and 37.36 px on Middlebury. PSMNet performs worst: 2.15 px on ETH3D, 3.77 px on KITTI 2012, and 48.62 px on Middlebury with 54.42% D1. These failures stem from fixed disparity range assumptions (e.g., PSMNet’s 192-pixel limit) and lack of semantic priors, making them unsuitable for cross-domain deployment.

2) *Method Selection: DEFOM as the Most Robust Choice:* Among all methods, **DEFOM demonstrates the most stable cross-domain performance.** Comparing EPE rankings across benchmarks: DEFOM ranks 4th on ETH3D (0.35 px), 2nd

on KITTI 2012 (0.84 px), 1st on KITTI 2015 (1.04 px), and 1st on Middlebury (4.65 px). While BridgeDepth achieves lower errors on ETH3D and KITTI, its Middlebury failure (20.03 px vs. DEFOM’s 4.65 px) reveals poor generalization to large disparity ranges. IGEV achieves best Middlebury D1 (6.79%) but shows higher EPE on KITTI datasets. DEFOM’s consistent top-tier performance across diverse scenarios—without catastrophic failures on any benchmark—makes it the safest choice for generating pseudo-ground-truth on unseen domains like our Tree Branches dataset.

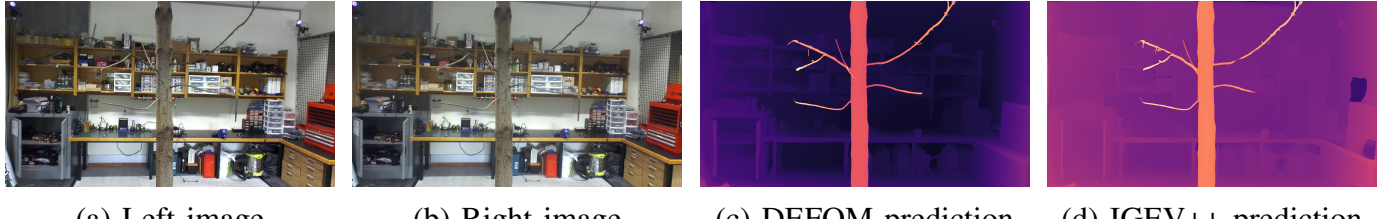


Fig. 2: Qualitative comparison on Scene 3305. DEFOM produces smoother disparity maps with better sky-region consistency. IGEV++ preserves finer branch details but exhibits noise in homogeneous areas.

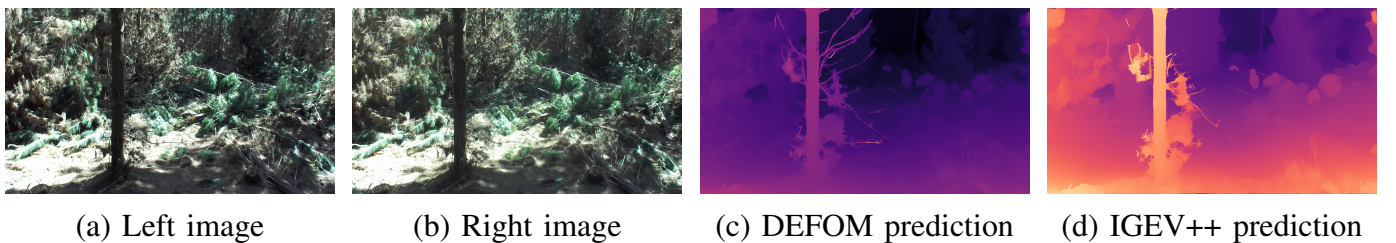


Fig. 3: Qualitative comparison on Scene 4939. DEFOM generates smooth depth transitions at occlusion boundaries. IGEV++ produces sharper edges but exhibits artifacts near thin structures.

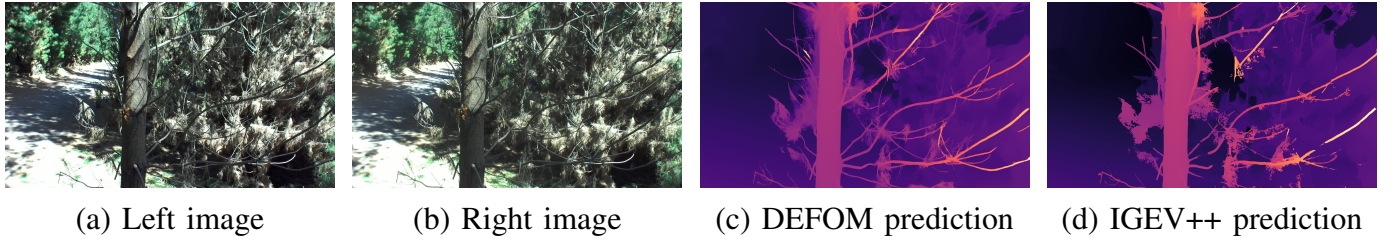


Fig. 4: Qualitative comparison on Scene 5128 under variable lighting conditions. DEFOM maintains stable depth predictions. IGEV++ shows more texture detail but less consistent depth.

B. Qualitative Evaluation on Tree Branches Dataset

Based on the benchmark analysis, we apply DEFOM to our Tree Branches dataset to generate pseudo-ground-truth depth maps. For comparison, we also evaluate IGEV++, which shows the best D1 among iterative methods on Middlebury (7.82%). Figs. 2–4 present qualitative comparisons on representative vegetation scenes.

Scene 3305 (Fig. 2): Dense foliage with overlapping branches. DEFOM produces spatially coherent disparity maps with consistent sky-region predictions. IGEV++ preserves finer branch details but exhibits noise in homogeneous areas.

Scene 4939 (Fig. 3): Extreme depth discontinuities. DEFOM generates clean depth transitions at occlusion boundaries. IGEV++ shows sharper edges but exhibits occasional artifacts near thin structures.

Scene 5128 (Fig. 4): Dappled illumination through canopy. DEFOM maintains stable predictions across shadow boundaries. IGEV++ produces more detailed texture but less consistent depth.

C. Establishing DEFOM as Gold Standard

Based on quantitative and qualitative evaluation, **DEFOM is selected as the gold-standard method** for generating pseudo-

ground-truth. Key factors: (1) top-2 EPE on 3 of 4 benchmarks without catastrophic failures; (2) smoother disparity maps with fewer artifacts on vegetation scenes; (3) stable performance across diverse domains.

V. DISCUSSION

A. Cross-Domain Generalization Analysis

Foundation models demonstrate superior cross-domain consistency through large-scale pretraining. **DEFOM achieves best ranked consistency** (average rank 1.75 across 4 benchmarks) with lowest CV (0.58), ideal for establishing reference baselines. BridgeDepth achieves lowest absolute error on ETH3D (0.23 px) but higher variance across domains.

DEFOM vs. IGEV++ Trade-offs: DEFOM excels in smoothness and consistency—essential for ground truth generation—achieving 31% lower EPE on Middlebury. IGEV++ offers better outlier control (D1: 7.82% vs. 8.28%), valuable for safety-critical detection but less suitable as reference baseline.

Critical Finding: Classical methods’ catastrophic failures (PSMNet: 54.42% D1 on Middlebury) versus modern methods’ stable performance demonstrates that architectural advances significantly improve cross-domain robustness.

B. Implications for Forestry Applications

DEFOM's selection as gold-standard baseline enables future quantitative evaluation without expensive LiDAR acquisition. Future work will validate against LiDAR measurements on selected scenes.

C. Limitations and Future Work

Limitations: (1) Tree Branches dataset evaluation is qualitative only; DEFOM's selection relies on cross-domain consistency and visual assessment. (2) Single-dataset training may not represent optimal generalization. (3) Statistical significance testing would strengthen comparative claims.

Future Directions: (1) Establish the Tree Branches dataset as a public benchmark with DEFOM pseudo-ground-truth. (2) Computational profiling for embedded UAV deployment. (3) Uncertainty quantification for safety-critical applications.

VI. CONCLUSION

This paper presented the first systematic zero-shot evaluation of deep stereo matching methods for UAV forestry applications. We evaluated eight methods spanning four architectural paradigms—iterative refinement, foundation models, diffusion-based, and 3D CNN—across four standard benchmarks and a novel 5,313-pair Tree Branches dataset.

Our evaluation revealed distinct cross-domain generalization patterns. Foundation models leveraging monocular depth priors achieved superior consistency, with DEFOM ranking 1st–2nd across all benchmarks (average rank 1.75). Iterative methods demonstrated moderate but stable performance, while classical 3D CNN methods exhibited catastrophic failures on out-of-distribution data, underscoring the importance of modern architectures for zero-shot deployment.

Based on these findings, we established DEFOM as the gold-standard baseline for generating pseudo-ground-truth on the Tree Branches dataset. This enables quantitative benchmarking of stereo methods on real-world vegetation scenes without expensive LiDAR annotation—addressing a critical need for developing autonomous UAV pruning systems that require centimeter-level depth accuracy.

The Tree Branches dataset, along with DEFOM pseudo-ground-truth, will be publicly released to facilitate future research in UAV-based forestry automation.

ACKNOWLEDGMENTS

This research was supported by the Royal Society of New Zealand Marsden Fund and the Ministry of Business, Innovation and Employment. We thank the forestry research stations for data collection access and our annotators for ground truth generation.

REFERENCES

- [1] N. Mayer, E. Ilg, P. Hausser, P. Fischer, D. Cremers, A. Dosovitskiy, and T. Brox, “A large dataset to train convolutional networks for disparity, optical flow, and scene flow estimation,” in *Proc. IEEE Conf. Comput. Vis. Pattern Recognit. (CVPR)*, 2016, pp. 4040–4048.
- [2] L. Lipson, Z. Teed, and J. Deng, “RAFT-Stereo: Multilevel recurrent field transforms for stereo matching,” in *Proc. Int. Conf. 3D Vis. (3DV)*, 2021, pp. 218–227.
- [3] G. Xu, X. Wang, X. Ding, and X. Yang, “Iterative geometry encoding volume for stereo matching,” in *Proc. IEEE Conf. Comput. Vis. Pattern Recognit. (CVPR)*, 2023, pp. 21919–21928.
- [4] G. Xu, X. Wang, Z. Zhang, J. Cheng, C. Liao, and X. Yang, “IGEV++: Iterative multi-range geometry encoding volumes for stereo matching,” *arXiv preprint arXiv:2409.00638*, 2024.
- [5] T. Guan, J. Guo, C. Wang, and Y.-H. Liu, “BridgeDepth: Bridging monocular and stereo reasoning with latent alignment,” *arXiv preprint arXiv:2508.04611*, 2025.
- [6] C. Zhao, Z. Zhang, M. Poggi, F. Tosi, Y. Guo, and S. Mattoccia, “Zero-shot stereo matching with diffusion models,” in *Proc. Eur. Conf. Comput. Vis. (ECCV)*, 2024, pp. 315–331.
- [7] H. Jiang, Z. Lou, L. Ding, R. Xu, M. Tan, W. Jiang, and R. Huang, “DEFOM-Stereo: Depth foundation model based stereo matching,” *arXiv preprint arXiv:2501.09466*, 2025.
- [8] A. Geiger, P. Lenz, and R. Urtasun, “Are we ready for autonomous driving? The KITTI vision benchmark suite,” in *Proc. IEEE Conf. Comput. Vis. Pattern Recognit. (CVPR)*, 2012, pp. 3354–3361.
- [9] M. Menze and A. Geiger, “Object scene flow for autonomous vehicles,” in *Proc. IEEE Conf. Comput. Vis. Pattern Recognit. (CVPR)*, 2015, pp. 3061–3070.
- [10] D. Scharstein, H. Hirschmüller, Y. Kitajima, G. Krathwohl, N. Nešić, X. Wang, and P. Westling, “High-resolution stereo datasets with subpixel-accurate ground truth,” in *Proc. German Conf. Pattern Recognit. (GCPR)*, 2014, pp. 31–42.
- [11] T. Schöps, J. L. Schönberger, S. Galliani, T. Sattler, K. Schindler, M. Pollefeys, and A. Geiger, “A multi-view stereo benchmark with high-resolution images and multi-camera videos,” in *Proc. IEEE Conf. Comput. Vis. Pattern Recognit. (CVPR)*, 2017, pp. 2538–2547.
- [12] D. Steininger, K. Roth, F. Tremer, F. Ehmann, H. K’oniger, M. Simon, and C. Trabelsi, “Timbervision: Towards a UAV-based forest monitoring system,” *IEEE Robot. Autom. Lett.*, vol. 10, no. 1, pp. 235–242, 2025.
- [13] Y. Lin, B. Xue, M. Zhang, S. Schofield, and R. Green, “Deep learning-based depth map generation and YOLO-integrated distance estimation for radiata pine branch detection using drone stereo vision,” in *Proc. Int. Conf. Image Vis. Comput. New Zealand (IVCNZ)*, Christchurch, New Zealand, 2024, pp. 1–6.
- [14] Y. Lin, B. Xue, M. Zhang, S. Schofield, and R. Green, “YOLO and SGBM integration for autonomous tree branch detection and depth estimation in radiata pine pruning applications,” in *Proc. Int. Conf. Image Vis. Comput. New Zealand (IVCNZ)*, Wellington, New Zealand, 2025, pp. 1–6.
- [15] Y. Lin, B. Xue, M. Zhang, S. Schofield, and R. Green, “Performance evaluation of deep learning for tree branch segmentation in autonomous forestry systems,” in *Proc. Int. Conf. Image Vis. Comput. New Zealand (IVCNZ)*, Wellington, New Zealand, 2025, pp. 1–6.
- [16] Y. Lin, B. Xue, M. Zhang, S. Schofield, and R. Green, “Genetic algorithms for parameter optimization for disparity map generation of radiata pine branch images,” in *Proc. Int. Conf. Image Vis. Comput. New Zealand (IVCNZ)*, Wellington, New Zealand, 2025, pp. 1–6.
- [17] D. Scharstein and R. Szeliski, “A taxonomy and evaluation of dense two-frame stereo correspondence algorithms,” *Int. J. Comput. Vis.*, vol. 47, no. 1–3, pp. 7–42, 2002.
- [18] Y. Boykov, O. Veksler, and R. Zabih, “Fast approximate energy minimization via graph cuts,” *IEEE Trans. Pattern Anal. Mach. Intell.*, vol. 23, no. 11, pp. 1222–1239, 2001.
- [19] P. F. Felzenswalb and D. R. Huttenlocher, “Efficient belief propagation for early vision,” *Int. J. Comput. Vis.*, vol. 70, no. 1, pp. 41–54, 2006.
- [20] H. Hirschmüller, “Stereo processing by semiglobal matching and mutual information,” *IEEE Trans. Pattern Anal. Mach. Intell.*, vol. 30, no. 2, pp. 328–341, 2008.
- [21] A. Kendall, H. Martirosyan, S. Dasgupta, P. Henry, R. Kennedy, A. Bachrach, and A. Bry, “End-to-end learning of geometry and context for deep stereo regression,” in *Proc. IEEE Int. Conf. Comput. Vis. (ICCV)*, 2017, pp. 66–75.
- [22] J.-R. Chang and Y.-S. Chen, “Pyramid stereo matching network,” in *Proc. IEEE Conf. Comput. Vis. Pattern Recognit. (CVPR)*, 2018, pp. 5410–5418.
- [23] F. Zhang, V. Prisacariu, R. Yang, and P. H. S. Torr, “GA-Net: Guided aggregation net for end-to-end stereo matching,” in *Proc. IEEE Conf. Comput. Vis. Pattern Recognit. (CVPR)*, 2019, pp. 185–194.
- [24] G. Xu, J. Cheng, P. Guo, and X. Yang, “Attention concatenation volume for accurate and efficient stereo matching,” in *Proc. IEEE Conf. Comput. Vis. Pattern Recognit. (CVPR)*, 2022, pp. 12981–12990.

- [25] F. Fraundorfer, L. Heng, D. Honegger, G. H. Lee, L. Meier, P. Tanskanen, and M. Pollefeys, "Vision-based autonomous mapping and exploration using a quadrotor MAV," in *Proc. IEEE/RSJ Int. Conf. Intell. Robots Syst. (IROS)*, 2012, pp. 4557–4564.
- [26] F. Nex and F. Remondino, "UAV for 3D mapping applications: A review," *Appl. Geomat.*, vol. 6, no. 1, pp. 1–15, 2014.
- [27] A. J. Barry and R. Tedrake, "Pushbroom stereo for high-speed navigation in cluttered environments," in *Proc. IEEE Int. Conf. Robot. Autom. (ICRA)*, 2015, pp. 3046–3052.
- [28] S. Jayathunga, T. Owari, and M. Tsuyuki, "Digital aerial photogrammetry for uneven-aged forest management: Assessing the potential to reconstruct canopy structure and estimate living biomass," *Remote Sens.*, vol. 11, no. 3, p. 338, 2019.
- [29] A. Tonioni, F. Tosi, M. Poggi, S. Mattoccia, and L. Di Stefano, "Real-time self-adaptive deep stereo," in *Proc. IEEE Conf. Comput. Vis. Pattern Recognit. (CVPR)*, 2019, pp. 195–204.
- [30] J. Watson, O. Mac Aodha, V. Prisacariu, G. Brostow, and M. Firman, "The temporal opportunist: Self-supervised multi-frame monocular depth," in *Proc. IEEE Conf. Comput. Vis. Pattern Recognit. (CVPR)*, 2021, pp. 1164–1174.